nature biotechnology

GFP-specific CD8 T cells enable targeted cell depletion and visualization of T-cell interactions

Judith Agudo[1], Albert Ruzo[1], Eun Sook Park[1], Robert Sweeney[1], Veronika Kana[2], Meng Wu[1], Yong Zhao[1], Dieter Egli[3], Miriam Merad[2,4,5] & Brian D Brown[1,4–6]

There are numerous cell types with scarcely understood functions, whose interactions with the immune system are not well characterized. To facilitate their study, we generated a mouse bearing enhanced green fluorescent protein (EGFP)-specific CD8$^+$ T cells. Transfer of the T cells into EGFP reporter animals can be used to kill EGFP-expressing cells, allowing selective depletion of desired cell types, or to interrogate T-cell interactions with specific populations. Using this system, we eliminate a rare EGFP-expressing cell type in the heart and demonstrate its role in cardiac function. We also show that naive T cells are recruited into the mouse brain by antigen-expressing microglia, providing evidence of an immune surveillance pathway in the central nervous system. The just EGFP death-inducing (Jedi) T cells enable visualization of a T-cell antigen. They also make it possible to utilize hundreds of existing EGFP-expressing mice, tumors, pathogens and other tools, to study T-cell interactions with many different cell types, to model disease states and to determine the functions of poorly characterized cell populations.

The surface of all nucleated cells contain major histocompatibility (MHC) class I molecules that present peptides from endogenously expressed proteins[1]. CD8$^+$ T cells scan the surface of cells, and engage only cells in which their T-cell receptor (TCR) has sufficient affinity for a specific peptide-MHC class I complex. The outcome of T-cell engagement is not only dependent on TCR affinity for the peptide-MHC complex, but also highly dependent on the nature of the cell presenting the antigen and the local mileu[2,3]. Although we know how T cells interact with some cell populations, T-cell interactions with many cell types, especially rare cell populations, have never been specifically studied[3].

The predominant means by which T-cell interactions with specific cell types have been studied is through the use of T cells engineered to express a TCR that recognizes a single peptide-MHC complex[4,5]. These models have been invaluable in advancing our understanding of immunology[6,7]. However, the study of T-cell interactions with their antigen-expressing targets has been limited by two factors in particular: technological difficulties in tracking and monitoring antigen-expressing cells and the lack of animals and reagents that express a model antigen in specific cell types.

Not only are there cell types whose interactions with the immune system are poorly studied, there are also cell populations whose functions have not been well characterized. This is also largely due to technological restrictions, in particular, the limitations of current methods to deplete specific cell populations. Depletion of a cell can be achieved using certain antibodies or by engineering mice to express the human diphtheria toxin receptor (DTR) under the control of a cell type–specific promoter and injecting diphtheria toxin (DT)[8,9]. However, there are relatively few depleting antibodies or DTR mice available, and repeated administration of the antibody or DT, which can be toxic, is required to stably deplete cell types that are quickly renewed, such as lymphocytes.

To address these challenges, we reasoned that EGFP could be used as a model antigen. EGFP is readily detected by flow cytometry and fluorescence microscopy, and there are hundreds of EGFP-expressing mice available[10], as well as EGFP-expressing cancer cell lines, viruses, bacteria and other tools. Here, we generated a mouse expressing an EGFP-specific TCR and show that this model enables wide-ranging studies of T-cell-tissue interactions and specific depletion of rare cell populations.

To generate mice expressing an EGFP-specific TCR, we used a somatic cell nuclear transfer (SCNT) approach[11]. The benefit of the SCNT approach is that the rearranged TCR is regulated at its endogenous locus and does not require the use of cultured T-cell clones. We crossed BALB/c and C57BL/6 mice, and immunized F_1 progeny mice (B6xBalbc) with a lentivirus encoding EGFP (LV.EGFP). After 2 weeks, we used a tetramer to isolate CD8$^+$ T cells expressing TCRs specific for the immunodominant epitope of EGFP ($EGFP_{200\text{-}208}$) presented on H-2K^d[12]. We directly used the cells as a nuclear donor for SCNT (**Fig. 1a**). We used B6xBalbc mice because SCNT is most efficient on a mixed background[11], and because we wanted the EGFP-specific T cells to recognize EGFP presented on H-2K^d. The H-2K^d allele enables a diverse use because BALB/c, nonobese diabetic (NOD) and NOD/severe combined immunodeficient (SCID) mice all have

[1]Department of Genetics and Genomic Sciences, Icahn School of Medicine at Mount Sinai, New York, New York, USA. [2]Department of Oncological Sciences, Icahn School of Medicine at Mount Sinai, New York, New York, USA. [3]The New York Stem Cell Foundation Research Institute, New York, New York, USA. [4]Mount Sinai Immunology Institute, Icahn School of Medicine at Mount Sinai, New York, New York, USA. [5]Tisch Cancer Institute, Icahn School of Medicine at Mount Sinai, New York, New York, USA. [6]Diabetes Obesity and Metabolism Institute, Icahn School of Medicine at Mount Sinai, New York, New York, USA. Correspondence should be addressed to B.D.B. (brian.brown@mssm.edu).

Received 28 April; accepted 23 September; published online 2 November 2015; doi:10.1038/nbt.3386

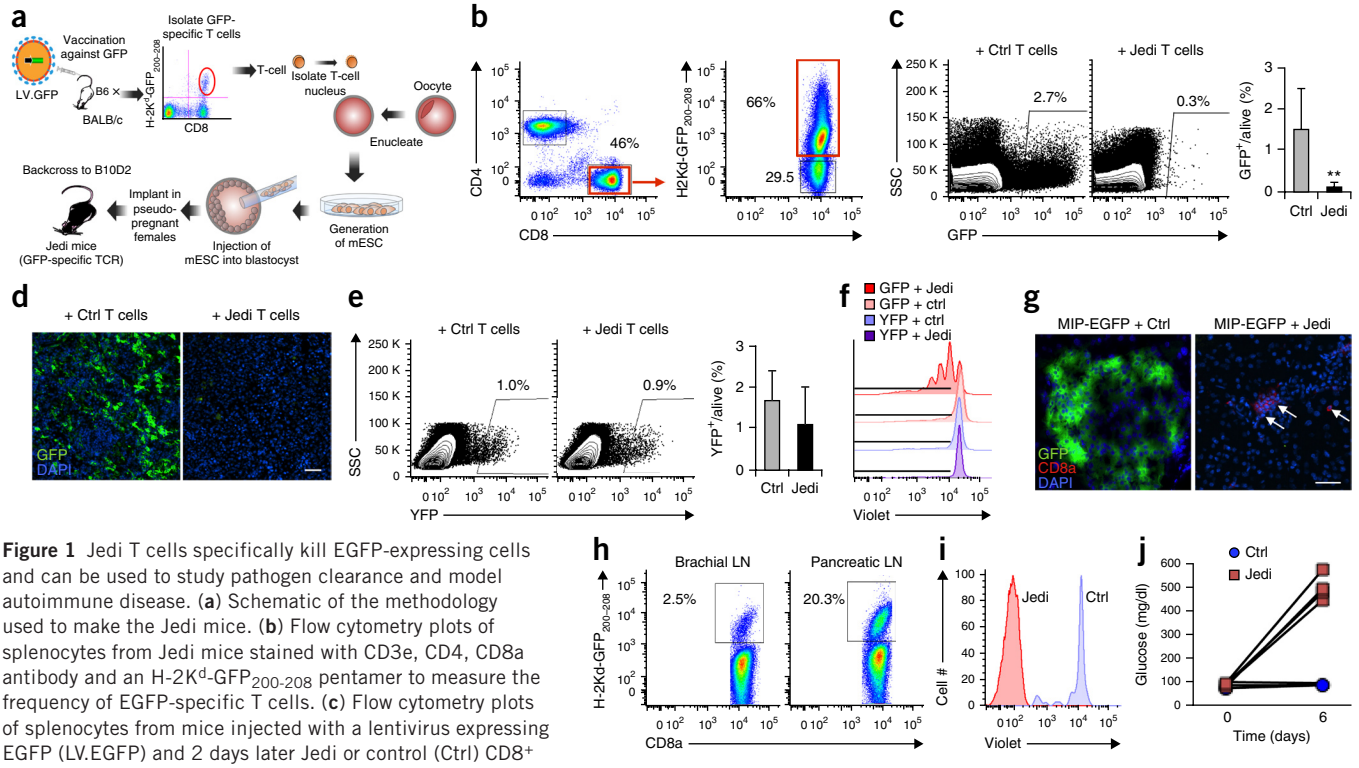

Figure 1 Jedi T cells specifically kill EGFP-expressing cells and can be used to study pathogen clearance and model autoimmune disease. (**a**) Schematic of the methodology used to make the Jedi mice. (**b**) Flow cytometry plots of splenocytes from Jedi mice stained with CD3e, CD4, CD8a antibody and an H-2K^d-GFP$_{200\text{-}208}$ pentamer to measure the frequency of EGFP-specific T cells. (**c**) Flow cytometry plots of splenocytes from mice injected with a lentivirus expressing EGFP (LV.EGFP) and 2 days later Jedi or control (Ctrl) CD8$^+$ T cells. Representative dot plot from two separate experiments showing percentage of EGFP-expressing cells 5 days after the LV.EGFP injection. Error bars, mean ± s.d. $n = 7$ mice/group. $^{**}P < 0.01$ versus control-treated (*t*-test). (**d**) Fluorescent microscopy analysis of the spleen of mice described in **c**. Representative images are shown. Scale bar, 100 µm. (**e**) Flow cytometry plots of splenoctyes from mice injected with LV.EYFP and 2 days later with Jedi or control CD8$^+$ T cells; shown are representative plots from two experiments, measuring EYFP-expressing cells 5 days after injection of LV.EYFP. Error bars in graph, mean ± s.d. $n = 3$ mice/group. (**f**) Representative flow cytometry plots of Jedi or Ctrl CD8+ T-cells stained with Violet Cell Proliferation dye and co-cultured with EGFP or EYFP expressing bone marrow-derived dendritic cells for 3 days. $n = 3$ wells/group. (**g**) Fluorescent microscopy analysis of the pancreas of MIP-EGFP mice 6 days after injection with Jedi or control CD8$^+$ T cells, and vaccination with EGFP. $n =$ 4 mice/group. Arrows point to CD8$^+$ cells in the tissue. Scale bar, 100 µm. (**h**) Flow cytometry of H-2K^d-GFP$_{200\text{-}208}$ pentamer positive CD8$^+$ T cells in the brachial and pancreatic lymph nodes of MIP-EGFP mice injected with Jedi T cells as in **g**. (**i**) Representative histogram of Violet Cell Proliferation dye-labeled Jedi T cells from pancreatic lymph nodes of MIP-EGFP mice 6 days after injection with Jedi or control CD8$^+$ T cells. $n = 2$ mice/group. (**j**) Blood glucose measurements at the indicated times of mice described in **g** ($n = 4$ mice/group).

the H-2K^d allele, and there are strains of C57BL mice with the H-2K^d haplotype, most notably B6D2 and B10D2. Therefore, any mouse model on the C57BL/6 strain can be bred with DBA or B10D2 mice, and all first-generation progeny will express the H-2K^d allele. In addition, knowledge of the immunodominant epitope presented on H-2K^d allows detection of EGFP-specific CD8$^+$ T cells with a tetramer. The F_1 mice were backcrossed for eight generations to B10D2 mice so that the mice (hereafter known as Jedi), expressed the H-2K^d allele and were on the C57BL background. More than 50% of CD8$^+$ T cells in all Jedi mice were specific for the GFP$_{200\text{-}208}$-H-2K^d pentamer, and their phenotype was naive (CD44$^-$CD62L$^+$) (**Fig. 1b** and **Supplementary Fig. 1**). PCR analysis and Sanger sequencing revealed that the rearranged TCR was Vα1-J30 and Vβ4-D1-J1.6-C1 (**Supplementary Fig. 2a**).

Monitoring antigen-expressing cells and their clearance by T cells is particularly relevant in viral immunology[13]. To determine if we could use our Jedi T cells to monitor removal of infected cells, we injected mice with LV.EGFP[14], or with an LV encoding yellow fluorescent protein (LV.EYFP), which has >95% homology to EGFP, but differs by one amino acid in the immunodominant epitope (**Supplementary Fig. 2b**). We then transferred CD8$^+$ T cells from the Jedi or control mice.

In mice that received control T cells, ~2% of splenocytes were EGFP$^+$, whereas in mice that received Jedi T cells, EGFP$^+$ cells were almost all eliminated, which indicated that Jedi T cells were capable of killing EGFP-expressing cells (**Fig. 1c,d**). In contrast, splenocytes from mice infected with LV.EYFP were not killed (**Fig. 1e**). To further assess the specificity of the Jedi T cells, we co-cultured them with dendritic cells expressing EGFP or EYFP and found that the T cells proliferated only in the presence of EGFP (**Fig. 1f** and **Supplementary Fig. 2c**). These results demonstrate the specificity and cytotoxic capacity of the Jedi T cells for EGFP-expressing cells.

Antigen-specific T cells have been used to model different autoimmune diseases[6]. A potential advantage of the Jedi T-cell approach over existing models is that it would enable qualitative and quantitative assessments at a cellular level, such as whether all target cells are killed. We set out to determine if we could use Jedi T cells to create a visualizable model of type I diabetes. We injected mice that express EGFP under the control of the mouse insulin promoter (MIP-EGFP)[15] with Jedi or control T cells and vaccinated them with EGFP to activate the transferred cells. Within 6 days of injecting Jedi T cells, we could not find any EGFP$^+$ beta-cells in the pancreas (**Fig. 1g**). Through analysis of EGFP$_{200\text{-}208}$-H-2K^d pentamer$^+$ cells, we found that the EGFP-specific T cells had primarily localized to the pancreatic draining lymph node (**Fig. 1h**) and undergone proliferation (**Fig. 1i**). Consistent with the loss of EGFP-expressing beta cells, MIP-EGFP mice that received Jedi T cells were diabetic, as indicated by their loss of glucose control (**Fig. 1j**).

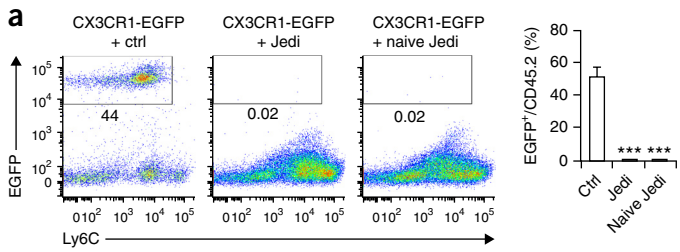

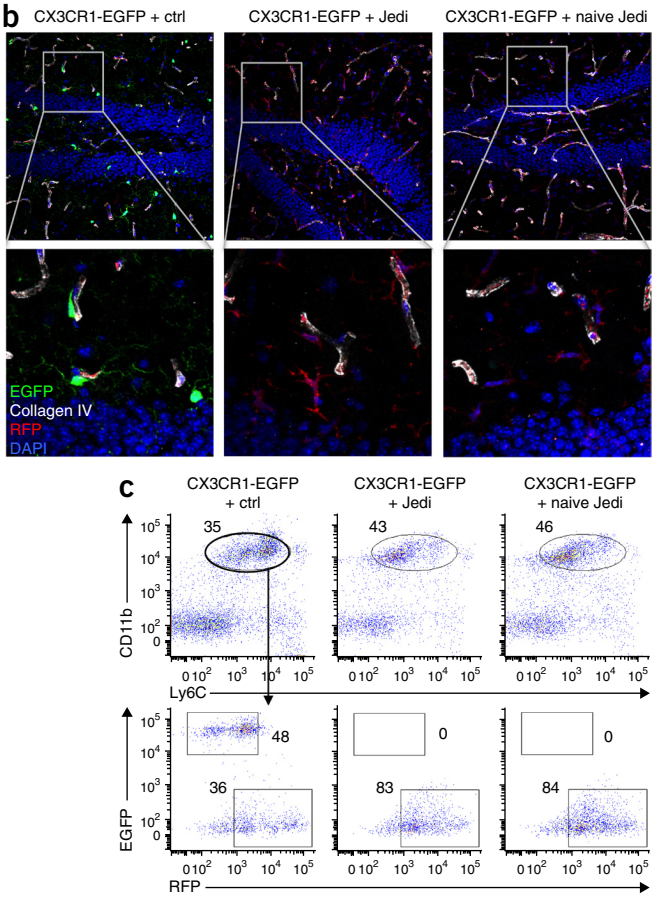

Figure 2 Jedi T cells reveal naive T cells can cross the BBB and kill antigen-expressing microglia. (**a**) Representative flow cytometry plots of EGFP-expressing microglia from CX3CR1-EGFP/actin-RFP chimeric mice 7 days after injection with Jedi or control CD8$^+$ T cells (left). Images labeled naive Jedi did not receive any EGFP vaccination. Graph represents , mean ± s.d. $n = 3$ mice/group. $^{***}P < 0.001$ versus control-treated (*t*-test) (right). (**b**) Representative images of the dentate gyrus of hippocampus 3 weeks after injection of the CD8$^+$ T cells and 13 weeks after bone marrow transplant. Collagen IV denotes vessel basement membrane. 20× magnification. (**c**) Flow cytometry plots of brain cells of CX3CR1-EGFP/actin-RFP chimeric mice after injection of Ctrl or Jedi CD8$^+$ T cells (as in **b**). Cells were analyzed 3 weeks after injection of the T cells to quantify the number of EGFP$^+$ and RFP$^+$ microglia (CD45^{int}Ly6c^{int}CD11b$^+$). Representative flow cytometry plots are shown from $n = 3$ mice/group.

Although tools are available to study antigen-dependent T-cell interactions with beta cells, those tools do not currently exist for many other cell types, such as, for microglia, brain-resident macrophages. It is unclear whether under brain homeostatic conditions CD8$^+$ T cells survey microglia, as the blood brain barrier (BBB) is believed to keep the brain mostly inaccessible to cellular infiltrates in the absence of inflammation[16]. To study the antigen-presenting capacity of microglia, we took advantage of the CX3CR1-EGFP mice[17], which express EGFP in microglia. Because CX3CR1 mice express EGFP also in circulating monocytes and some other myeloid cells, we used bone marrow transplant to create chimeric mice with EGFP$^+$ microglia, and red fluorescent protein (RFP) peripheral hematopoietic cells. To do this, we lethally irradiated the CX3CR1-EGFP mice, which ablated all the peripheral myeloid cells but spared microglia since they are radioresistant[18], and transplanted bone marrow from actin-RFP mice into the irradiated recipients. After 10 weeks, the hematopoietic cells in the periphery were all RFP$^+$ and EGFP$^-$, indicating that engraftment of the actin-RFP cells was complete, but the microglia were still EGFP$^+$ (**Supplementary Fig. 3a–c**).

We transferred Jedi or control CD8$^+$ T cells into the CX3CR1-EGFP/actin-RFP mice 10 weeks after the bone marrow transplant, a time by which the BBB has been fully repaired from irradiation and is not even permissible to serum albumin[19]. After transfer the mice were either vaccinated with EGFP or left unvaccinated to keep the T cells naive. Remarkably, within 1 week all of the EGFP$^+$ microglia were eliminated from mice that received Jedi T cells, even those that were not vaccinated (**Fig. 2a**,**b** and **Supplementary Fig. 3d**). This was concomitant with the presence of Jedi T cells, but not control T cells, in the brain (**Supplementary Fig. 3e**,**f**). The EGFP$^+$ microglia remained absent after 3 weeks, but there were RFP$^+$ macrophages (CD45^{int}Ly6c^{int}CD11b$^+$) in the brain (**Fig. 2b**,**c**), which is consistent with previous reports that peripheral monocytes can replace microglia after injury[20,21] and extends this observation to the context of CD8$^+$ T-cell-mediated clearance.

These findings indicate that naive T cells can enter the brain when microglia present an antigen recognized by the T cells and suggest the existence of an immune surveillance pathway for the brain that is mediated by microglia. Further work will be necessary to better understand the mechanisms involved. In particular, it will be relevant to determine if other antigen-presenting cells play a role through cross-presentation of antigen derived from the microglia. It will also be important to confirm our findings in a model in which irradiation was not used because we cannot rule out the possibility that irradiation had somehow altered the BBB.

The rapid clearance of EGFP-expressing microglia and beta cells by the Jedi T cells led us to reason that these cells may also have utility as a method for depleting cells to study their function.

We first tested whether we could copy the phenotype of an established cell depletion model using Jedi T cells. We selected Foxp3$^+$ regulatory T cells (T_{reg} cells) as a target because the phenotype of T_{reg} cell depletion is known[22], although whether CD8$^+$ T cells could kill T_{reg} cells was unknown. In addition, T_{reg} cells are a renewing population so we could use this model to assess the stability of cell depletion. To determine if Jedi T cells could be used to deplete T_{reg} cells, we injected Foxp3-EGFP mice with Jedi or control T cells. In Foxp3-EGFP mice, EGFP has been knocked in to the Foxp3 gene on the X chromosome[23]. We initially injected heterozygous female Foxp3-EGFP mice. Due to random X-inactivation ~50% of the T_{reg} cells were Foxp3$^+$EGFP$^+$, and the other 50% were Foxp3$^+$EGFP$^-$ (**Fig. 3a**). Within 6 days of injecting activated Jedi T cells, there was a complete elimination of Foxp3$^+$EGFP$^+$ cells (**Fig. 3a**,**b**). The Foxp3$^+$EGFP$^-$ cells were not depleted but instead increased in numbers to compensate for the loss of the EGFP$^+$ T_{reg} cells. Depletion was maintained for up to 14 days (the last time assessed) without any need to transfer more T cells or to revaccinate (**Fig. 3b**), and the frequency of Jedi T cells contracted to very low levels (**Fig. 3c**).

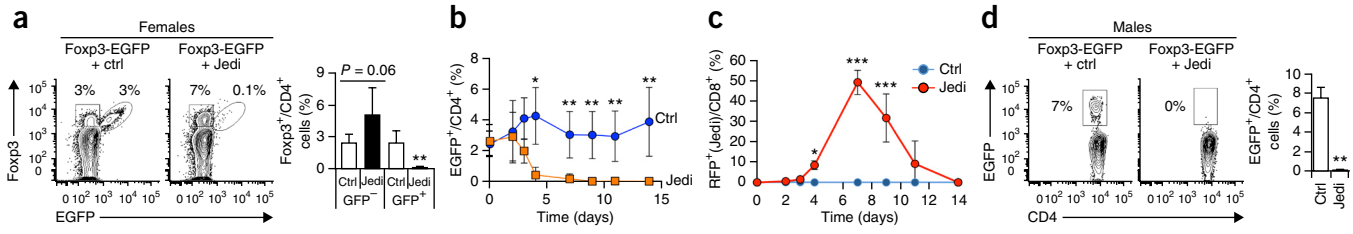

Figure 3 Jedi T cells can stably deplete a renewing cell population to study their function. (**a**) Representative flow cytometry analysis and quantification of the frequency of EGFP$^+$ Foxp3$^+$ cells in lymph nodes of Foxp3-EGFP females 15 days after injection of Jedi or Ctrl CD8$^+$ T cells and vaccinated with EGFP. Cells were stained with CD3e, CD4, CD25 and Foxp3 to mark regulatory T cells ($n = 5$ mice/group). Graph presents mean ± s.d. $^{**}P < 0.01$ versus control-treated (*t*-test). (**b**) Percentage of EGFP$^+$ cells among CD4$^+$ T cells from Foxp3-EGFP female mice injected with either control (Ctrl) or Jedi T cells. $n = 5$ mice/group. Graph presents mean ± s.d. $^*P < 0.05$, $^{**}P < 0.01$, $^{***}P < 0.01$ vs. control-treated (*t*-test). (**c**) Percentage of Jedi T cells among CD8$^+$ T cells was determined in the blood at the indicated time points from the mice described in **b** ($n = 5$ mice/group). The Jedi mice and control littermates were transgenic actin-RFP (red fluorescent protein). (**d**) Flow cytometry analysis of the frequency of EGFP$^+$ cells in the brachial lymph node 10 days after Foxp3-EGFP male mice were injected with either control or Jedi T cells and vaccinated with EGFP. $n = 3$–4 mice/group. Graph presents mean ± s.d. $^{**}P < 0.01$ vs. control-treated (*t*-test). (**e**) Representative image of the face of Foxp3-EGFP mice (treated as in **d**) showing conjunctivitis in the Jedi-treated mice (left) and image of the brachial, axillary and inguinal lymph nodes and the spleen taken from control-treated and Jedi-treated Foxp3-EGFP mice 10 days after adoptive transfer (right) ($n = 3$–4 mice/group). Scale bar, 1 cm.

Next, we injected male Foxp3-EGFP mice in which all Foxp3$^+$ cells are EGFP$^+$. Within 6 days there was complete depletion of Foxp3$^+$EGFP$^+$ T_{reg} cells (**Fig. 3d** and **Supplementary Fig. 4a**,**b**). By 10 days all the Jedi-treated Foxp3-EGFP mice had become ill and showed clear indications of immune dysregulation, including conjunctivitis, splenomegaly, enlarged lymph nodes and expansion of neutrophils (**Fig. 3e** and **Supplementary Fig. 4c**), consistent with the phenotype of T_{reg}-depleted mice[22]. We investigated the influence of T-cell dosage on target cell depletion by injecting Foxp3-EGFP male mice with 5×10^4, 1.5×10^5, or 5×10^5 CD8$^+$ Jedi T cells. At the two highest cell doses, EGFP$^+$ cells were completely eliminated in all Foxp3-EGFP mice injected. At the lowest cell dose, EGFP$^+$ cells were eliminated in two out of three mice; in one mouse the Jedi T cells did not expand, and EGFP$^+$ cells were not eliminated (**Supplementary Fig. 4d**,**e**). Thus, there appears to be a cell dose threshold for efficient killing, which is likely to depend on the nature of the EGFP-expressing mouse model.

To determine if we could use the Jedi to eliminate a rare cell population in a nonlymphoid organ, we targeted Hcn4$^+$ cells. These cells are found in the heart and are extremely rare; there are <10,000 Hcn4$^+$ cells in a mouse[24]. They are known to be involved in pacemaking, but there are conflicting reports regarding the overall importance of Hcn4$^+$ cells in cardiac function[25,26]. We injected Hcn4-EGFP mice[24], which express EGFP under the control of the Hcn4 promoter, with Jedi or control T cells, and vaccinated them with EGFP. Within 5 days we could detect CD8$^+$ T cells localizing with EGFP$^+$ cells in the heart (**Fig. 4a**). Pentamer staining indicated that these cells were Jedi T cells (**Fig. 4b**). Strikingly, by 10 days the Hcn4-EGFP cells were entirely

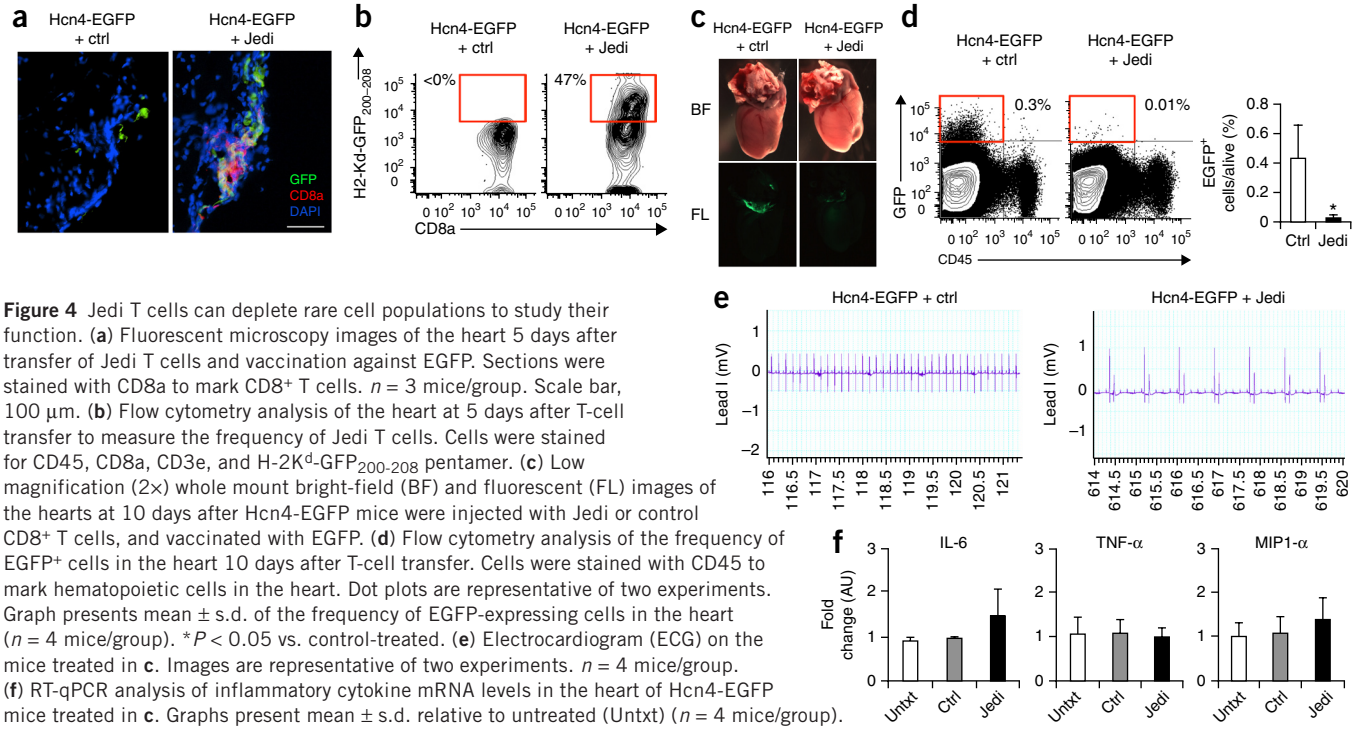

Figure 4 Jedi T cells can deplete rare cell populations to study their function. (**a**) Fluorescent microscopy images of the heart 5 days after transfer of Jedi T cells and vaccination against EGFP. Sections were stained with CD8a to mark CD8$^+$ T cells. $n = 3$ mice/group. Scale bar, 100 µm. (**b**) Flow cytometry analysis of the heart at 5 days after T-cell transfer to measure the frequency of Jedi T cells. Cells were stained for CD45, CD8a, CD3e, and H-2K^d-GFP$_{200\text{-}208}$ pentamer. (**c**) Low magnification (2×) whole mount bright-field (BF) and fluorescent (FL) images of the hearts at 10 days after Hcn4-EGFP mice were injected with Jedi or control CD8$^+$ T cells, and vaccinated with EGFP. (**d**) Flow cytometry analysis of the frequency of EGFP$^+$ cells in the heart 10 days after T-cell transfer. Cells were stained with CD45 to mark hematopoietic cells in the heart. Dot plots are representative of two experiments. Graph presents mean ± s.d. of the frequency of EGFP-expressing cells in the heart ($n = 4$ mice/group). $^*P < 0.05$ vs. control-treated. (**e**) Electrocardiogram (ECG) on the mice treated in **c**. Images are representative of two experiments. $n = 4$ mice/group. (**f**) RT-qPCR analysis of inflammatory cytokine mRNA levels in the heart of Hcn4-EGFP mice treated in **c**. Graphs present mean ± s.d. relative to untreated (Untxt) ($n = 4$ mice/group).

absent from the heart of the Hcn4-EGFP mice injected with Jedi T cells (**Fig. 4c**). Unlike in other depletion technologies, we were able to assess target cell depletion at single-cell resolution using flow cytometry and confirm that the Jedi T cells completely eliminated the $Hcn4^+$ cells from the hearts (**Fig. 4d**).

We then performed an electrocardiogram (ECG) on the mice after depletion of $Hcn4^+$ cells to determine the outcome of depletion on cardiac function. Whereas mice injected with control T cells had a normal ECG, all mice injected with Jedi T cells had bradycardia and atrioventricular block (**Fig. 4e** and **Supplementary Fig. 5**). This was not due to immune cell infiltration or inflammation because after 10 days there was no evidence of increased T cells or pro-inflammatory cytokines in the hearts of the mice (**Fig. 4f**). These findings support the role of $Hcn4^+$ cells in cardiac conduction and pacemaking. They also demonstrate that Jedi T cells can home to and kill EGFP-expressing cells even in nonlymphoid, noninflamed tissue, and provide a means of targeted cell depletion.

There are many areas of immunological research where the Jedi will be particularly valuable because with them one can visualize the antigen and take advantage of the numerous existing EGFP-expressing reagents. These include identifying tolerogenic or immune-privileged cell types, testing cell-targeted vaccines, monitoring T-cell trafficking to antigen-expressing cells in normal and diseased tissues, studying T-cell interactions with particular cell types and cell states within a primary and metastatic tumor, and for identifying cytotoxic T-lymphocyte-resistant cancer cells, which will be greatly facilitated by the ability to sort surviving cells by flow cytometry. It will also be possible to use the Jedi to create novel models of tissue autoimmunity and organ rejection, and for studying pathogen clearance, in a manner more accessible to state-of-the-art imaging, including live cell imaging. In addition to their relevance for basic biology, these applications of the Jedi will also facilitate target discovery and preclinical testing of immune modulatory drugs.

This work additionally demonstrates that Jedi T cells can be used for targeted cell depletion. The main advantages of this approach over existing cell depletion methods, such as the DTR system, are the ability to easily assess the elimination of the target cells using EGFP, the stability of depletion and the greater availability of cell type–specific EGFP-expressing models. Indeed, there are more than 1,000 different EGFP-expressing mice (e.g., **Supplementary Table 1**), many of which express EGFP in populations whose functions are not well characterized[10,27]. We also note that Jedi T cell–mediated killing is a physiological method of cell depletion, as this is the natural function of $CD8^+$ T cells. For this reason, there are mechanisms to control excessive tissue damage by T cells[28]. This is evident by the absence of inflammation and the contraction of the $CD8^+$ T cells after antigen-expressing cells are cleared. For studies in which cell ablation is used to study tissue repair, T-cell-mediated depletion may better approximate physiological conditions as one of the causes of tissue regeneration is T-cell-mediated clearance of cells.

For the studies performed here we adoptively transferred $CD8^+$ Jedi T cells, usually ~10^6, and vaccinated the recipient mice to activate and expand the Jedi T cells. This was done to maximize the killing potential. However, the Jedi mouse could be bred directly with cell type–specific EGFP-expressing mice, or mice in which EGFP expression is inducible, as an alternative approach. For applications in which transient depletion is desired, the Jedi mice could be engineered to express a suicide gene, such as DTR, so that the Jedi T cells can be conditionally depleted. Because Jedi T cells recognize EGFP presented on H-$2K^d$, they can be used in NOD/SCID-based mouse models, including human xenograft models. These applications of the Jedi mouse will enable dissection of the mechanisms by which T cells interact with discreet cell populations in different contexts at a very granular level, and help determine the function of cell types that have remained poorly characterized.

METHODS

Methods and any associated references are available in the online version of the paper.

Note: Any Supplementary Information and Source Data files are available in the online version of the paper.

ACKNOWLEDGMENTS

We thank A. Annoni, L. Sherman, J. Brody, J. Lafaille, S. Lira, J. Blander and M. Feldmann for helpful discussions. We also thank K. Kelly and the Mouse Genetics and Mouse Targeting facility, and A. Rahman and the Flow Cytometry Core for technical assistance. B.D.B. and M.M. were supported by US National Institutes of Health (NIH) R01AI104848 and R01AI113221. B.D.B. was also supported by a Pilot Award from the Diabetes Research, Obesity and Metabolism Institute and an Innovation Award from the Juvenile Diabetes Research Foundation (JDRF). Y.Z. was supported by NIH1R01HL107376. J.A. was supported by the Robin Chemers Neustein Award, and a JDRF postdoctoral fellowship. V.K. was supported by a Swiss National Foundation Early Postdoc Mobility fellowship.

AUTHOR CONTRIBUTIONS

J.A. designed and performed experiments, analyzed data and wrote the manuscript, A.R., E.S.P., R.S. M.W. and V.K. performed experiments or acquired data, Y.Z. analyzed data, D.E. performed experiments, M.M. designed experiments, analyzed data, and edited the manuscript, B.D.B. designed and supervised the research, analyzed data and wrote the manuscript.

COMPETING FINANCIAL INTERESTS

The authors declare no competing financial interests.

1. Pamer, E. & Cresswell, P. Mechanisms of MHC class I–restricted antigen processing. *Annu. Rev. Immunol.* **16**, 323–358 (1998).
2. Fletcher, A.L., Malhotra, D. & Turley, S.J. Lymph node stroma broaden the peripheral tolerance paradigm. *Trends Immunol.* **32**, 12–18 (2011).
3. Mueller, S.N. & Germain, R.N. Stromal cell contributions to the homeostasis and functionality of the immune system. *Nat. Rev. Immunol.* **9**, 618–629 (2009).
4. Kisielow, P., Blüthmann, H., Staerz, U.D., Steinmetz, M. & von Boehmer, H. Tolerance in T-cell-receptor transgenic mice involves deletion of nonmature CD4+8+ thymocytes. *Nature* **333**, 742–746 (1988).
5. Clarke, S.R. *et al.* Characterization of the ovalbumin-specific TCR transgenic line OT-I: MHC elements for positive and negative selection. *Immunol. Cell Biol.* **78**, 110–117 (2000).
6. Lafaille, J.J. T-cell receptor transgenic mice in the study of autoimmune diseases. *J. Autoimmun.* **22**, 95–106 (2004).
7. Berg, L.J. *et al.* Antigen/MHC-specific T cells are preferentially exported from the thymus in the presence of their MHC ligand. *Cell* **58**, 1035–1046 (1989).
8. Saito, M. *et al.* Diphtheria toxin receptor-mediated conditional and targeted cell ablation in transgenic mice. *Nat. Biotechnol.* **19**, 746–750 (2001).
9. Jung, S. *et al. In vivo* depletion of CD11c+ dendritic cells abrogates priming of $CD8^+$ T cells by exogenous cell-associated antigens. *Immunity* **17**, 211–220 (2002).
10. Schmidt, E.F., Kus, L., Gong, S. & Heintz, N. BAC transgenic mice and the GENSAT database of engineered mouse strains. *Cold Spring Harb. Protoc.* doi:10.1101/pdb.top073692 (1 March 2013).
11. Kirak, O. *et al.* Transnuclear mice with predefined T cell receptor specificities against Toxoplasma gondii obtained via SCNT. *Science* **328**, 243–248 (2010).
12. Gambotto, A. *et al.* Immunogenicity of enhanced green fluorescent protein (EGFP) in BALB/c mice: identification of an H2-Kd-restricted CTL epitope. *Gene Ther.* **7**, 2036–2040 (2000).
13. Norbury, C.C., Malide, D., Gibbs, J.S., Bennink, J.R. & Yewdell, J.W. Visualizing priming of virus-specific $CD8^+$ T cells by infected dendritic cells *in vivo*. *Nat. Immunol.* **3**, 265–271 (2002).
14. Agudo, J. *et al.* The miR-126-VEGFR2 axis controls the innate response to pathogen-associated nucleic acids. *Nat. Immunol.* **15**, 54–62 (2014).
15. Hara, M. *et al.* Transgenic mice with green fluorescent protein-labeled pancreatic beta-cells. *Am. J. Physiol. Endocrinol. Metab.* **284**, E177–E183 (2003).
16. Engelhardt, B. & Ransohoff, R.M. Capture, crawl, cross: the T cell code to breach the blood-brain barriers. *Trends Immunol.* **33**, 579–589 (2012).

17. Jung, S. *et al.* Analysis of fractalkine receptor CX(3)CR1 function by targeted deletion and green fluorescent protein reporter gene insertion. *Mol. Cell. Biol.* **20**, 4106–4114 (2000).
18. Ransohoff, R.M. & Cardona, A.E. The myeloid cells of the central nervous system parenchyma. *Nature* **468**, 253–262 (2010).
19. Sándor, N. *et al.* Low dose cranial irradiation-induced cerebrovascular damage is reversible in mice. *PLoS One* **9**, e112397 (2014).
20. Ajami, B., Bennett, J.L., Krieger, C., McNagny, K.M. & Rossi, F.M.V. Infiltrating monocytes trigger EAE progression, but do not contribute to the resident microglia pool. *Nat. Neurosci.* **14**, 1142–1149 (2011).
21. Yamasaki, R. *et al.* Differential roles of microglia and monocytes in the inflamed central nervous system. *J. Exp. Med.* **211**, 1533–1549 (2014).
22. Kim, J.M., Rasmussen, J.P. & Rudensky, A.Y. Regulatory T cells prevent catastrophic autoimmunity throughout the lifespan of mice. *Nat. Immunol.* **8**, 191–197 (2007).
23. Fontenot, J.D. *et al.* Regulatory T cell lineage specification by the forkhead transcription factor foxp3. *Immunity* **22**, 329–341 (2005).
24. Wu, M., Peng, S. & Zhao, Y. Inducible gene deletion in the entire cardiac conduction system using Hcn4-CreERT2 BAC transgenic mice. *Genesis* **52**, 134–140 (2014).
25. Herrmann, S., Hofmann, F., Stieber, J. & Ludwig, A. HCN channels in the heart: lessons from mouse mutants. *Br. J. Pharmacol.* **166**, 501–509 (2012).
26. Bucchi, A., Barbuti, A., Difrancesco, D. & Baruscotti, M. Funny current and cardiac rhythm: insights from HCN knockout and transgenic mouse models. *Front. Physiol.* **3**, 240 (2012).
27. Gong, S. *et al.* A gene expression atlas of the central nervous system based on bacterial artificial chromosomes. *Nature* **425**, 917–925 (2003).
28. Parish, I.A. *et al.* Tissue destruction caused by cytotoxic T lymphocytes induces deletional tolerance. *Proc. Natl. Acad. Sci. USA* **106**, 3901–3906 (2009).

ONLINE METHODS

Mice. B10D2, BALB/c, CD45.1 (B6/SJL), actin-RFP and MIP-EGFP[15] mice were purchased from Jackson Laboratories. Foxp3-EGFP mice[23] and CX3CR1-EGFP mice[17] were from established colonies. Hcn4-EGFP mice were generated by Y.Z. and M.W[24]. Because Jedi T cells recognize $EGFP_{200\text{-}208}$ presented on H-$2K^d$, all mouse experiments were done with either B10D2 or in F_1 progeny of B10D2 crossed to the indicated EGFP-expressing mouse. All experiments were performed when mice were 6–10 weeks-old and both male and females were used. Mice were randomly distributed minimizing the bias for cage, gender and age between groups. Investigators were not blinded to the groups. All animal procedures were performed according to protocols approved by the Mount Sinai School of Medicine Institutional Animal Care and Use Committee.

Generation of Jedi mice by somatic cell nuclear transfer (SCNT[11]). C57BL/6 and BALB/c mice were bred to generate mix background F_1 mice. The mice were vaccinated against EGFP by intravenous injection of 3×10^8 transducing units of a lentiviral vector encoding EGFP. Two weeks later livers and spleens were harvested for T-cell isolation. Briefly, livers and spleens were mechanically disrupted and filtered through a 70-µm cell strainer (Fisherbrand) to obtain a single-cell suspension. A Percoll gradient was used to enrich the leukocyte fraction from the livers. After red blood cell lysis using multispecies RBC lysis buffer (eBiosciences) for 2 min, cells were stained with $GFP_{200\text{-}208}$-$H2K^d$ APC labeled pentamer (ProImmune) following the manufacturer's instructions. T cells were further stained with CD8 (53-6.7)-PerCPCy5.5, CD4 (RM4-5)-APC-Alexa 788, CD3e (145-2C11)-PE and B220 (RA3-6B2)-FITC (eBiosciences). $GFP_{200\text{-}208}$-$H2K^d$-positive $CD8^+$ T cells were purified by sorting using Aria 5LS (BD Biosciences) and directly frozen in 10% DMSO 20% FBS-supplemented DMEM (Life Technologies).

For nuclear transfer into mouse oocytes, T cells were thawed, washed with DMEM with 10% FBS to remove DMSO, and then kept on ice in a volume of 25–50 µl. Mouse oocytes were obtained from 6- to 8-week-old $B6D2F_1$/J females (Jackson Laboratories strain 100006) by injecting 5–10 IU of pregnant mare serum (PMS), followed by injection of 5–10 IU of human chorionic gonadotropin (hCG) 48–52 h after PMS injection. Oocytes were retrieved 13–14 h after hCG injection, denuded using bovine hyaluronidase, and kept in KSOM (Millipore) until transfer. Nuclear transfer manipulations were done essentially as described[29]. In brief, oocytes were enucleated in GMOPS (G-3-(*N*-morpholino)propanesulfonic acid) plus containing 4 µg/ml cytochalasinB. T cells were aspirated into a microinjection pipette of 5 µm diameter (Humagen Piezo-15-5), applying piezo pulses at an intensity of 1–2 to lyse the plasma membrane of the T cell. T cells were then injected into the enucleated mouse oocyte using a piezo pulse at intensity 1–2, followed by removal of the plasma membrane surrounding the injected site to prevent lysis. At 1–3 h after transfer, oocytes were activated using strontium chloride for 90 min, with the addition of cytochalasin B at 5 µg/ml for 5 h. The histone deacetylation inhibitor scriptaid was added at a concentration of 250 ng/ml for 12 h to enhance reprogramming efficiency[30]. After 4 days of culture, the zona pellucida was removed from blastocysts, and the blastocysts were plated in mouse embryonic stem cell medium consisting of KO-DMEM, 12% KO-SR, NEAA, Glutamax, beta mercaptoethanol (all reagents from LifeTechnologies) and LIF (Millipore) on a mouse embryonic fibroblast feeder layer (GlobalStem). Embryonic stem cell outgrowths were picked manually, then passaged enzymatically using TrypLE (Life Technologies).

The SCNT-derived embryonic stem cells were injected into blastocysts from mice on the C57BL/6 background and implanted into pseudo-pregnant female CD1 mice by the Mouse Genetics and Mouse Targeting facility in Icahn School of Medicine at Mount Sinai. Jedi mice were genotyped by PCR using the following primers: TCRα Fw: GAGGAGCCAGCAGAAGGT; TCRα Rev: TCCCACCCTACACTCACTACA; TCRβ Fw: TCAAGTCGCTTCCAACCTCAA; TCRβ Rev: TGTCACAGTGAGCCGGGTG.

T-cell adoptive transfer. $CD8^+$ T cells were purified from spleens and lymph nodes (cranial, axillar, brachial, inguinal and mesenteric) of Jedi and control littermates by mechanical disruption and filtering through 70-µm cell strainer. After RBC lysis, $CD8^+$ T cells were negatively selected using the mouse $CD8^+$ T cells isolation kit II from Miltenyi following manufacturer's instructions. 5×10^5–5×10^6 Jedi or control T cells were transferred per mouse by tail vein injection. For activation of T cells, recipient mice were injected i.v. with $1–2 \times 10^8$ transducing units of a vesicular stomatitis virus (VSV)-pseudotyped lentiviral vectors encoding green fluorescent protein (LV.EGFP).

Infection with EYFP and EGFP-encoding lentivirus. B10D2 mice received 3×10^8 TU of lentivirus encoding either enhanced yellow fluorescent protein (EYFP) or EGFP. Three days later Jedi or control littermate cells were adoptively transferred. The lentivirus were produced as previously described[31]. Briefly, third-generation packaging plasmids along with transfer plasmids encoding EGFP or EYFP were transfected into 293T cells by $Ca_3(PO_4)_2$ transfection. Supernatants containing the vector were collected, passed through a 0.22-µm filter, and vectors were concentrated by ultracentrifugation. Titers were estimated as TU/ml on 293T cells by flow cytometry analysis of EYFP-positive or EGFP-positive 293T cells.

T-cell proliferation *in vitro*. Bone marrow was harvested from B10D2 mice by flushing tibiae and femurs with media, lysing RBCs and plating the remaining cells in RPMI 1640 media supplemented with 20 ng/ml of GM-CSF (Peprotech). The cells were transduced with either LV.EGFP or LV.EYFP overnight at day 1 at a multiplicity of infection (MOI) of 100. GM-CSF-supplemented media was added at day 3 of culture. $CD8^+$ T cells were isolated as described above and stained with Brilliant Violet proliferation dye eFluor450 dye (Invitrogen) following the manufacturer's instructions.

Glucose measurement and measurement of $EGFP^+$ T_{reg} cells and Jedi cells in blood. Glucose levels were determined from a drop of blood obtained by clipping the tail using OneTouch Ultra glucometer. All mice were tested in fed condition and no restrainer was used. To detect Jedi or $EGFP^+$ cells in the blood, in a similar fashion, a drop of blood from the tail was collected in 2 mM EDTA 1% BSA PBS. After red blood cells lysis, as described above, cells were stained and analyzed by flow cytometry.

Bone marrow transplant. C57BL/6 CX3CR1-EGFP x B10D2 mice were lethally irradiated (2× 600 rad, 3 h apart using a cesium source) and 4 h later were injected with 5 million bone marrow cells isolated from CD45.2 actin-RFP × B10D2 mice.

Immunofluorescence. Spleens, pancreata and hearts were harvested and frozen directly in OCT, 8-µm sections were taken and were fixed for 5 min with cold acetone prior to staining. Brains were fixed in 4% paraformaldehyde (Sigma-Aldrich), equilibrated in 20% sucrose (Sigma-Aldrich) and embedded in OCT prior to sectioning. 10-µm sagittal brain sections were incubated with 2% goat serum, 1% BSA, Fc-Block 1:1,000, 0.05% Tween-20 and 0.1% Triton X-100 in PBS before staining and stained in 1% goat serum, 1% BSA, 0.5% Triton X-100, Fc-Block 1:1,000. RFP staining was performed with mouse RFP (GT1610) antibody (Abcam) and a secondary goat anti-mouse AF-568 (Life Technologies). Vessels in the brain were stained with rabbit anti-collagen IV, polyclonal (BioRad, #2150-1470) and a secondary goat anti-rabbit AF-647 (Life Technologies). T-cell staining was performed for 2 h with either Alexa Fluor 594-conjugated anti-CD8a (clone 53-6.7 BioLegend) or CD3e staining with Alexa Fluor 647-conjugated anti-CD3a (clone 17A2 BioLegend) and DAPI (Vector Laboratories) for nuclei labeling. Sections from heart and pancreata were blocked with 2% rat serum and 0.5% BSA in PBS before staining with Alexa Fluor 594-conjugated anti-CD8a. Images were obtained with an upright wide-field microscope (Nikon) equipped with a 20× lens, and analyzed with NisElements software, or with an Zeiss LSM 780 confocal microscope and analyzed with ZEN (Zeiss) and ImageJ softwares.

Electrocardiography. For surface electrocardiography, mice were anesthetized with 1.75% isoflurane at a core temperature of 37 °C. Needle electrodes (AD Instruments) were placed subcutaneously in standard limb lead configurations. Signals were sampled using a PowerLab16/30 interface (AD Instruments). Data analysis was performed using LabChart (v 7.3.7, AD Instruments).

Flow cytometry analysis. Spleen and lymph nodes were digested in Hank's buffered salt solution (HBSS) (Invitrogen) containing 10% FBS and 0.2 mg/ml

collagenase IV (Sigma-Aldrich) for 15 min at 37 °C. After filtration using 70-µm cell strainer (Fisherbrand) to obtain a single-cell suspension, red blood cells (RBC) in the spleen were lysed with RBC lysis buffer (eBioscience) for 3 min. Brains were similarly digested; a Percoll gradient was used for the isolation of hematopoietic cells previous to the RBC lysis. Briefly, for the brain, single-cell suspensions were resuspended in a 37% Percoll (GE Healthcare) and underlayed by a 60% Percoll solution. The samples were then centrifuged at 600*g* for 20 min. Hearts were digested in 1 mg/ml collagenase IV in 10% FBS HBSS for 30 min at 37 °C and similarly filtered through a 70-µM cell strainer and RBC were lysed for 3 min.

The gating strategy used for the flow cytometry analysis is shown in the **Supplementary Figure 6**. Samples were stained with: CD45 (30-$F_1$1) APC-Alexa780, CD8 (53-6.7)-PerCPCy5.5, CD4 (RM4-5)-APC and eFluro450, CD3e (145-2C11)-PE, H2-Kb (AF6-88.5.5.3)-APC, H2-K_d (SF_1-1.1.1)-PE, CD25 (PC6.1)-PerCP-Cy5.5, FoxP3 (FJK-16s)-APC, CD11b (M1/70)-PerCP-Cy5.5 and Gr1 (RB6-8C5) PE from eBioscience. DAPI (Sigma-Aldrich) was used to stain dead cells. LSR-Fortessa and LSR-II (BD Biosciences) were used to acquire the samples and FlowJo was used to analyze the data.

mRNA expression analysis. For measuring cytokine expression in tissue, hearts were collected from mice and immediately frozen in dry ice for later processing. For RNA extraction, tissue was homogenized in Trizol (Qiagen) by mechanical disruption by using the Tissue Disruptor (Qiagen) and the RNA was then extracted following the manufacturer's instructions. 0.1-1 µg total RNA was reverse-transcribed for 1 h at 37 °C using RNA-to-cDNA kit (Applied Biosystems). qPCR was performed using the SYBR green qPCR master mix 2× (Fermentas, Thermo Scientific) and the following primers:

Actin Fw: ctaaggccaaccgtgaaaag, actin Rev: accagaggcatacagggaca;

IL6 Fw: TGATGGATGCTACCAAACTGG; IL6 Rev: TTCATGTACTCC AGGTAGCTATGG;

MIP1α Fw: CAAGTCTTCTCAGCGCCATA; MIP1α Rev: GGAATCT TCCGGCTGTAGG;

TNF Fw: CTGTAGCCCACGTCGTAGC; TNF Rev: TTTGAGATCCA TGCCGTTG.

TCR sequencing. To obtain the specific alpha and beta sequences of the Jedi T cells, splenocytes from a Jedi mouse were stained with a CD3e-PE, CD8a-FITC antibodies and $GFP_{200\text{-}208}$-$H2K^d$ APC pentamer as described above. Pentamer$^+$ CD8 T cells were FACS-sorted in Influx Cell Sorter (BD Biosciences) and resuspended in Trizol. RNA was isolated as described above. 5′RACE (Invitrogen) was performed following the manufacturer's instructions to amplify the alpha and beta regions. A 3′ primer recognizing the constant region in alpha and the constant region in beta were used, respectively. The DNA fragment obtained was cloned into a TOPO plasmid (Invitrogen) following the manufacturer's instructions and submitted to sequencing by Sanger method. Cα primer: TGGCGTTGGTCTCTTTGAAG; Cβ primer; CCAGAAGGTAGCAGAGACCC.

Statistical analysis. No prespecified effect size was used to determine sample sizes. Differences between groups were compared by independent two tailed Student's *t*-test for unequal variances. $P < 0.05$ was considered statistically significant.

29. Egli, D. & Eggan, K. Nuclear transfer into mouse oocytes. *J. Vis. Exp.* **1**, 116 (2006).
30. Van Thuan, N. *et al.* The histone deacetylase inhibitor scriptaid enhances nascent mRNA production and rescues full-term development in cloned inbred mice. *Reproduction* **138**, 309–317 (2009).
31. Brown, B.D. *et al.* Endogenous microRNA can be broadly exploited to regulate transgene expression according to tissue, lineage and differentiation state. *Nat. Biotechnol.* **25**, 1457–1467 (2007).

doi:10.1038/nbt.3386